

# Positive and Unlabeled Data: Model, Estimation, Inference, and Classification

Siyang Liu<sup>1</sup>, Chi-Kuang Yeh<sup>2</sup>, Xin Zhang<sup>3</sup>, Qinglong Tian<sup>2</sup>, and Pengfei Li<sup>2</sup>

<sup>1</sup>East China Normal University

<sup>2</sup>University of Waterloo

<sup>3</sup>Iowa State University

July 18, 2024

## Abstract

This study introduces a new approach to addressing positive and unlabeled (PU) data through the double exponential tilting model (DETM). Traditional methods often fall short because they only apply to selected completely at random (SCAR) PU data, where the labeled positive and unlabeled positive data are assumed to be from the same distribution. In contrast, our DETM's dual structure effectively accommodates the more complex and underexplored selected at random PU data, where the labeled and unlabeled positive data can be from different distributions. We rigorously establish the theoretical foundations of DETM, including identifiability, parameter estimation, and asymptotic properties. Additionally, we move forward to statistical inference by developing a goodness-of-fit test for the SCAR condition and constructing confidence intervals for the proportion of positive instances in the target domain. We leverage an approximated Bayes classifier for classification tasks, demonstrating DETM's robust performance in prediction. Through theoretical insights and practical applications, this study highlights DETM as a comprehensive framework for addressing the challenges of PU data.

*Keywords:* Density ratio, Empirical likelihood, Exponential tilting model, Mixture model,

Out-of-distribution detection, Transfer learning

# 1 Introduction

## 1.1 Positive and Unlabeled Data

Considering a binary response variable  $Y \in \{0, 1\}$  and features  $\mathbf{X} \in \mathbb{R}^p$ , positive and unlabeled (PU) data refer to datasets that consist of the following two samples: The first sample is labeled, but all observations have positive responses  $y = 1$ ; the second sample contains both positive ( $y = 1$ ) and negative ( $y = 0$ ) instances. However, the second sample is unlabeled, meaning we can only access the features  $\mathbf{x}$  but have no access to their labels  $y$ . PU data are prevalent in many areas, including biomedical study, ecology, and machine learning.

**Contaminated Case-Control Data** A case-control study is a research design widely used in biomedical research to investigate the causes of diseases. It compares two groups: a group of patients with the disease (the case group) and a group of healthy people (the control group). Data contamination is a common issue in case-control studies. For example, the underdiagnosis phenomenon refers to a situation where the false positive rate is very low, and the case group can generally be seen as pure and only contains patients. However, some medical conditions may go unrecognized in many patients, and they are misclassified as healthy ones. Then, many people in the control group are, in fact, patients. For example, Begg (1994) and Godley and Schell (1999) highlighted an issue in a prostate cancer study, indicating that 20%-40% of the control group consists of latent prostate cancer cases, rendering the control group contaminated. In the underdiagnosis example, the case group can be seen as a positive-only sample, but the contaminated control group is an unlabeled sample containing both positive and negative cases because we do not know who are real healthy people and patients.

**Presence-Only Data** Presence-only data can come from various fields, including ecology, epidemiology, and marketing. For example, ecological studies often rely on presence-only data to model a species' habitat (Ward et al. 2009). The dataset comprises two samples: one contains confirmed presence locations of a species obtained through field surveys or other methods; the other contains locations sampled from the full study area. However, the presence status of the species in the latter sample is unknown. Thus, the first sample is positive only while the second sample contains both presence and non-presence locations but is unlabeled, meaning that we do not know which location has the confirmed presence of the species.

**PU Data in Machine Learning** PU data are commonly seen in many machine learning tasks. For instance, on an online video streaming platform, users click on videos that they find interesting. However, for videos that are not clicked, it is uncertain whether users are interested in them or not, as users may ignore those videos while browsing. In such a scenario, those clicked videos are positive-only data, while unclicked videos are considered unlabeled data for a recommendation system. In computer vision, tasks like facial recognition are often based on PU data. Take this specific example: We aim to identify a user from various images using some known reference pictures of that person. Here, the labeled sample comprises all clearly identified face images of that user. The unlabeled sample we wish to identify consists of photos of the user and others. We refer interested readers to read Jaskie and Spanias (2019) for more examples of PU data in machine learning.

## 1.2 Notation and Motivations

Using the terminologies from transfer learning, we consider a source domain  $p_s(\mathbf{x}, y)$  and a target domain  $p_t(\mathbf{x}, y)$ . In the rest of this paper, we use the generic notation  $p_s(\cdot)$  (and  $\text{Pr}_s(\cdot)$ ) and  $p_t(\cdot)$  (and  $\text{Pr}_t(\cdot)$ ) to denote densities (and probabilities) on the source and target domains, respectively. The labeled positive data are sampled from the source domain

$$\{(\mathbf{x}_i, y_i = 1), i = 1, \dots, n\} \sim p_s(\mathbf{x}|y = 1).$$

The unlabeled data are from the target domain

$$\{\mathbf{x}_i, i = n + 1, \dots, n + m\} \sim p_t(\mathbf{x}). \quad (1)$$

The marginal distribution of  $\mathbf{X}$  in (1) can be seen as a mixture distribution

$$p_t(\mathbf{x}) = \pi p_t(\mathbf{x}|y = 1) + (1 - \pi)p_t(\mathbf{x}|y = 0),$$

where  $\pi$  is the mixture proportion  $\pi \equiv \text{Pr}_t(y = 1)$  of positive cases in the target domain.

Even though much research has been done on PU data, most of it suffers from two major limitations. The first limitation is that many existing works require the mixture proportion  $\pi$  to be known. However, such an assumption is usually unrealistic as  $\pi$  is rarely known. Even with prior knowledge of mixture proportion, one must use an estimate to replace the underlying true value. However, it is generally unclear how the difference between the estimated and true values will affect the analysis results.

The second major limitation is that most existing research works are constrained to the selected completely at random (SCAR) PU data (Bekker and Davis 2020), which imposes the assumption that  $p_s(\mathbf{x}|y = 1) = p_t(\mathbf{x}|y = 1)$ . The SCAR assumption has been widely used for simplicity: one of the mixture components,  $p_t(\mathbf{x}|y = 1)$ , is readily identifiable because the positive-only data  $\{(\mathbf{x}_i, y_i = 1), i = 1, \dots, n\}$  are from the same distribution

as  $p_t(\mathbf{x}|y = 1)$ . Despite its popularity, the SCAR assumption does not always reflect the true underlying data-generating mechanism. For example, in the contaminated case-control study example, it is reasonable to believe that the latent prostate cancer cases were misdiagnosed as healthy ones not only because of bad luck but also because their disease symptoms were not as severe as patients in the case group (i.e.,  $p_s(\mathbf{x}|y = 1) \neq p_t(\mathbf{x}|y = 1)$ ).

As opposed to the SCAR assumption, the selected at random (SAR) PU setting (Bekker and Davis 2020) allows  $p_s(\mathbf{x}|y = 1)$  to be different from  $p_t(\mathbf{x}|y = 1)$ , thus it can better reflect the true data-generating mechanism. Figure 1 shows the difference between SCAR and SAR PU data. However, despite its flexibility, the SAR PU setting presents numerous challenges, the foremost being the identifiability of the distributions of unlabeled positive and unlabeled negative data (i.e.,  $p_t(\mathbf{x}|y = 1)$  and  $p_t(\mathbf{x}|y = 0)$ ).

The aim of this paper is to relax the SCAR assumption and model PU data under the SAR setting. In addition, we aim to propose a method that does not rely on prior knowledge of the mixture proportion  $\pi$ .

### 1.3 Related Work and Challenges

PU data have been studied under different names in the statistical literature, including contaminated case-control data (e.g., Qin and Lawless 1994; Lancaster and Imbens 1996; Qin 1999; Qin and Liang 2011; Duan et al. 2020) and presence-only data (e.g., Ward et al. 2009; Song and Raskutti 2019). However, the aforementioned works are constrained under the SCAR assumption and often rely on knowing the true value of the mixture proportion. One exception is Wang et al. (2021), where they consider the SAR setting. However, they further require a smaller labeled verification sample from the target distribution. Thus, data from their setting cannot be seen as PU data.

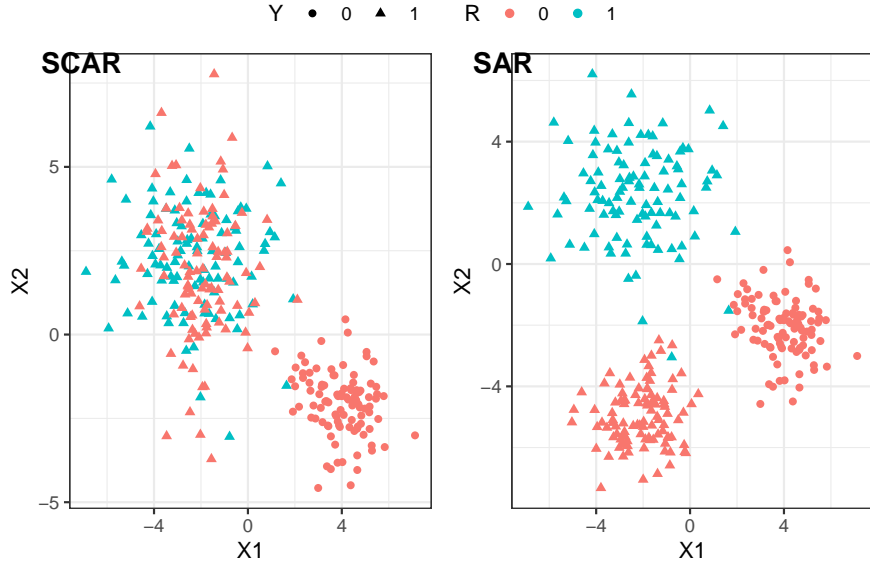


Figure 1: We use  $R = 0$  (red) and  $R = 1$  (blue), respectively, to denote data from the target and source. In the SCAR setting, the labeled positive (blue triangles) and unlabeled positive (red triangles) are from the same distribution. However, they may be different in the SAR setting.

In machine learning literature, most works on PU data focus on the SCAR assumption (e.g., Elkan and Noto 2008; Ramaswamy et al. 2016; Garg et al. 2021). However, a few works try to address the SAR setting. Kato et al. (2019) impose an “invariance of order” assumption, which states that, for observations in the labeled source data, the higher the probability  $\Pr_s(y = 1|\mathbf{x})$  is, the closer it is to the unlabeled positive distributing  $p_t(\mathbf{x}|y = 1)$ . In addition, their method requires the mixture proportion  $\pi = \Pr_t(y = 1)$  to be known. Bekker et al. (2019) propose a method similar to inverse probability weighting, which requires estimating the propensity score function. To ensure identifiability, they assume that the propensity score function needs to depend on fewer features than the predictive model (i.e., the shadow variable assumption in the missing data literature). Coudray et al. (2023) further establish risk bounds based on Bekker et al. (2019). Nevertheless, the shadow

variables are generally unknown, let alone their existence, thus reducing the method’s applicability. Gong et al. (2021) follow a similar framework as in Bekker et al. (2019) but do not impose the shadow variable assumption. However, they require a highly restrictive assumption that the propensity score function has a value of less than 0.5 for all observations from the unlabeled data under the logistic regression model. Furmańczyk et al. (2022) use a similar idea as Bekker et al. (2019) and Gong et al. (2021), in which they prove the model identifiability under logistic regression. However, their prediction approach requires that the positive and negative instances in the unlabeled data are separable. In addition, existing works on the SAR PU setting focus solely on classification (i.e., prediction) and do not address statistical inference. Problems like the the goodness-of-fit of the SCAR condition, and inference of the mixture proportion are remained unexplored.

## 1.4 Our Contributions and Overview

In this paper, we propose a new model, called the double exponential tilting model (DETM), for the SAR PU data, and prove that it is identifiable. Based on the proposed model, we develop an Expectation-Maximization (EM) algorithm for estimating parameters using the empirical likelihood (EL) method. It is worth noting that our method works even if the mixture proportion is unknown. Lastly, we apply the proposed model to address inference and prediction tasks, including model selection, confidence intervals, hypothesis testing, and classification. The highlights of our contributions are summarized in the following.

- Our proposed model, based on modeling the density ratios, is identifiable up to label switching. With some further mild assumptions, the model becomes fully identifiable.
- We propose a simple EM algorithm for estimating parameters, including the mixture proportion and odds ratios.

- We investigate the asymptotic behavior of our proposed estimator and propose hypothesis testing procedures for the mixture proportion and the goodness-of-fit of the SCAR condition.
- We use an approximated Bayes classifier based on the proposed model for classification tasks on the target domain.
- We implement the proposed methods in a R package, PUEM, which is available in the supplementary materials.

The rest of this paper is organized as follows. Section 2 introduces the proposed DETM. Section 3 discusses how to estimate parameters under the proposed model. Section 4 establishes theoretical results for statistical inference and classification. Section 5 examines the empirical performance of the proposed methods using simulation studies and real data application. We close the paper with concluding remarks given in Section 6. All the technical details and proofs are given in the supplementary materials.

## 2 Model

### 2.1 Density Ratio is the Key

A commonly used strategy in distributional shift problems (or, broadly speaking, transfer learning) for connecting the source and target domains is to utilize the density ratio. For example, adjusting the covariate shift often relies on estimating the density ratio of the features  $\mathbf{x}$  in the target and source domains (e.g., Shimodaira 2000; Sugiyama et al. 2007), and adjusting the label shift often requires estimating the density ratio of the response in the target and source domains (e.g., Lipton et al. 2018; Tian et al. 2023; Kim et al. 2024).



The aforementioned works on transfer learning suggest that modeling the density ratios is a promising direction for solving the SAR PU problem, which also involves a source and a target domain and belongs to the broad concept of transfer learning. In fact, examining the Bayes classifier for the target domain also reveals the key role of the density ratios. The Bayes classifier utilizes the posterior probability of the label and is optimal because it minimizes the prediction risk. The Bayes classifier on the target domain is defined as

$$\mathcal{C}(\mathbf{x}) = \mathbb{1} \{ \Pr_t(Y = 1 | \mathbf{X} = \mathbf{x}) > 0.5 \},$$

where  $\mathbb{1}(\cdot)$  is the indicator function. We can rewrite  $\Pr_t(Y = 1 | \mathbf{X})$  using the Bayes rule as

$$\Pr_t(Y = 1 | \mathbf{X} = \mathbf{x}) = \frac{p_t(\mathbf{x}, y = 1)}{p_t(\mathbf{x})} = \frac{\pi p_t(\mathbf{x} | y = 1)}{\pi p_t(\mathbf{x} | y = 1) + (1 - \pi) p_t(\mathbf{x} | y = 0)}.$$

We can further write  $\Pr_t(Y = 1 | \mathbf{X})$  by dividing both the numerator and denominator by  $p_s(\mathbf{x} | y = 1)$ :

$$\Pr_t(Y = 1 | \mathbf{X} = \mathbf{x}) = \frac{\pi \Lambda_1(\mathbf{x})}{\pi \Lambda_1(\mathbf{x}) + (1 - \pi) \Lambda_2(\mathbf{x})}, \quad (2)$$

where  $\Lambda_1(\mathbf{x})$  and  $\Lambda_2(\mathbf{x})$  are density ratios and are defined as

$$\Lambda_1(\mathbf{x}) \equiv \frac{p_t(\mathbf{x} | y = 1)}{p_s(\mathbf{x} | y = 1)} \quad \text{and} \quad \Lambda_2(\mathbf{x}) \equiv \frac{p_t(\mathbf{x} | y = 0)}{p_s(\mathbf{x} | y = 1)}.$$

Equation (2) implies that the Bayes classifier hinges on the mixture proportion  $\pi$  and two density ratios  $\Lambda_1(\mathbf{x})$  and  $\Lambda_2(\mathbf{x})$ . This finding also points out that it is promising to model the SAR PU data using the density ratios.

## 2.2 Identifiability Problem

We have underscored the importance of  $\Lambda_1(\mathbf{x})$  and  $\Lambda_2(\mathbf{x})$  in the previous section. However, we will show that if  $\Lambda_1(\mathbf{x})$  and  $\Lambda_2(\mathbf{x})$  are unconstrained,  $\pi$ ,  $\Lambda_1(\mathbf{x})$ , and  $\Lambda_2(\mathbf{x})$  are non-identifiable.

The unlabeled data are from the distribution  $p_t(\mathbf{x})$ , which can be rewritten as

$$\begin{aligned} p_t(\mathbf{x}) &= \pi p_t(\mathbf{x}|y=1) + (1-\pi)p_t(\mathbf{x}|y=0) \\ &= p_s(\mathbf{x}|y=1) \{ \pi \Lambda_1(\mathbf{x}) + (1-\pi) \Lambda_2(\mathbf{x}) \}. \end{aligned} \tag{3}$$

The left side of (3) (i.e.,  $p_t(\mathbf{x})$ ) is identifiable because we have the unlabeled target data  $\{\mathbf{x}_i, i = n+1, \dots, n+m\}$ . For the right side,  $p_s(\mathbf{x}|y=1)$  is also identifiable because we have access to the labeled source data  $\{(\mathbf{x}_i, y_i = 1), i = 1, \dots, n\}$ . Thus, the model identifiability depends on  $\pi \Lambda_1(\mathbf{x}) + (1-\pi) \Lambda_2(\mathbf{x})$ .

However, for any  $\pi^* \in (0, 1)$  that satisfies  $\pi^* < \pi$ , we have the following equation

$$\pi \Lambda_1(\mathbf{x}) + (1-\pi) \Lambda_2(\mathbf{x}) = \pi^* \Lambda_1(\mathbf{x}) + (1-\pi^*) \Lambda_2^*(\mathbf{x}),$$

where

$$\Lambda_2^*(\mathbf{x}) \equiv \frac{\pi - \pi^*}{1 - \pi^*} \Lambda_1(\mathbf{x}) + \frac{1 - \pi}{1 - \pi^*} \Lambda_2(\mathbf{x}).$$

Here  $\Lambda_2^*(\mathbf{x})$  is also a density ratio function because it satisfies  $\int \Lambda_2^*(\mathbf{x}) p_s(\mathbf{x}|y=1) d\mathbf{x} = 1$  and  $\Lambda_2^*(\mathbf{x}) \geq 0$ . Therefore, both  $\{\pi^*, \Lambda_1(\mathbf{x}), \Lambda_2^*(\mathbf{x})\}$  and  $\{\pi, \Lambda_1(\mathbf{x}), \Lambda_2(\mathbf{x})\}$  satisfy (3). In other words,  $\pi$ ,  $\Lambda_1(\mathbf{x})$ , and  $\Lambda_2(\mathbf{x})$  are non-identifiable if we do not further impose more assumptions.

### 2.3 Double Exponential Tilting Model

Previous discussions reveal that we must impose some constraints on  $\Lambda_1(\mathbf{x})$  and  $\Lambda_2(\mathbf{x})$  to solve the identifiability issue. The exponential tilting model (ETM) is a popular choice for modeling the density ratios. For example, Maity et al. (2023) used the ETM to model the density ratio between the source and target domains in a transfer learning setting. Also, the ETM is widely used in areas such as case-control studies (e.g., Qin 1998; Qin and Liang 2011; Qin 2017).

Based on previous discussions, we use the ETM to connect the source and target domains. Rather than using an exponential tilting model for  $p_t(\mathbf{x}, y)/p_s(\mathbf{x}, y)$  (e.g., Maity et al. 2023), we acknowledge that the target distribution  $p_t(\mathbf{x})$  is a mixture of  $p_t(\mathbf{x}|y = 1)$  and  $p_t(\mathbf{x}|y = 0)$ . Thus, we connect the source sample distribution  $p_s(\mathbf{x}|y = 1)$  with the two mixture components  $p_t(\mathbf{x}|y = 1)$  and  $p_t(\mathbf{x}|y = 0)$  using two ETMs separately. We call our proposed model the DETM, where the details are given below.

We impose the ETM to both  $\Lambda_1(\mathbf{x})$  and  $\Lambda_2(\mathbf{x})$  as follows.

$$\log \{\Lambda_1(\mathbf{x})\} = \alpha_1 + \mathbf{x}^T \boldsymbol{\beta}_1, \quad \log \{\Lambda_2(\mathbf{x})\} = \alpha_2 + \mathbf{x}^T \boldsymbol{\beta}_2, \quad (4)$$

where  $\Lambda_1(\mathbf{x})$  and  $\Lambda_2(\mathbf{x})$  are given by

$$\Lambda_1(\mathbf{x}) = \frac{p_t(\mathbf{x}|y = 1)}{p_s(\mathbf{x}|y = 1)} \quad \text{and} \quad \Lambda_2(\mathbf{x}) = \frac{p_t(\mathbf{x}|y = 0)}{p_s(\mathbf{x}|y = 1)}.$$

In the DETM in (4),  $\alpha_1$  and  $\alpha_2$  are two normalizing constants such that the two density ratios must satisfy

$$\int \Lambda_1(\mathbf{x}) p_s(\mathbf{x}|y = 1) d\mathbf{x} = 1 \quad \text{and} \quad \int \Lambda_2(\mathbf{x}) p_s(\mathbf{x}|y = 1) d\mathbf{x} = 1. \quad (5)$$

We use a linear combination  $\mathbf{x}^T \boldsymbol{\beta}$  in (4), and one can generally replace  $\mathbf{x}$  with a known function of  $\mathbf{T}(\mathbf{x})$ . For example, we can use a polynomial function  $\mathbf{T}(x) = (x, x^2, x^3)$  to increase the model’s flexibility. For high-dimensional features such as images, we can use the embedding layer of a pre-trained neural network as  $\mathbf{T}(\mathbf{x})$ . We will continue to use  $\mathbf{x}^T \boldsymbol{\beta}$  to facilitate presentations in the rest of the paper.

The remaining question is to address the identifiability of the DETM. As we have shown in (3), the key to model identifiability lies in  $\pi \Lambda_1(\mathbf{x}) + (1 - \pi) \Lambda_2(\mathbf{x})$ . In the next theorem, we prove that  $\pi \Lambda_1(\mathbf{x}) + (1 - \pi) \Lambda_2(\mathbf{x})$  is “almost” identifiable and can become fully identifiable with some mild assumptions. The proof is given in the supplementary materials.

**Theorem 1** (Identifiability). *Under the DETM in (4), we model the density ratios as  $\Lambda_1(\mathbf{x}) = \exp(\alpha_1 + \mathbf{x}^T \boldsymbol{\beta})$  and  $\Lambda_2(\mathbf{x}) = \exp(\alpha_2 + \mathbf{x}^T \boldsymbol{\beta})$ , and we let  $\pi = \Pr_t(Y = 1)$ . If  $(\pi, \alpha_1, \boldsymbol{\beta}_1, \alpha_2, \boldsymbol{\beta}_2)$  and  $(\pi^*, \alpha_1^*, \boldsymbol{\beta}_1^*, \alpha_2^*, \boldsymbol{\beta}_2^*)$  satisfy*

$$\pi \exp(\alpha_1 + \mathbf{x}^T \boldsymbol{\beta}_1) + (1 - \pi) \exp(\alpha_2 + \mathbf{x}^T \boldsymbol{\beta}_2) = \pi^* \exp(\alpha_1^* + \mathbf{x}^T \boldsymbol{\beta}_1^*) + (1 - \pi^*) \exp(\alpha_2^* + \mathbf{x}^T \boldsymbol{\beta}_2^*),$$

*for any  $\mathbf{x} \in \mathbb{R}^p$ , then the two sets of parameters are either the same*

$$(\pi, \alpha_1, \boldsymbol{\beta}_1, \alpha_2, \boldsymbol{\beta}_2) = (\pi^*, \alpha_1^*, \boldsymbol{\beta}_1^*, \alpha_2^*, \boldsymbol{\beta}_2^*)$$

*or subject to label switching*

$$(\pi, \alpha_1, \boldsymbol{\beta}_1, \alpha_2, \boldsymbol{\beta}_2) = (1 - \pi^*, \alpha_2^*, \boldsymbol{\beta}_2^*, \alpha_1^*, \boldsymbol{\beta}_1^*).$$

**Remark 1.** *Theorem 1 reveals that the DETM is identifiable up to exchanging the label  $Y$ .*

*The label switching issue is inherent in the model specification in (4) due to the symmetry of  $\Lambda_1(\mathbf{x})$  and  $\Lambda_2(\mathbf{x})$ . We can achieve full model identifiability by introducing some reasonable assumptions to solve the label-switching problem. For instance, if positive cases are less frequent in the unlabeled dataset (e.g., misdiagnosis is rare), we can impose the condition  $\pi < 0.5$ , which resolves the label-switching problem. Alternatively, if we believe the labeled positive source distribution  $p_s(\mathbf{x}|y = 1)$  is more similar to the positive target distribution  $p_t(\mathbf{x}|y = 1)$  than the negative target distribution  $p_t(\mathbf{x}|y = 0)$ , we can impose an assumption based on some distance measure, such as the Kullback-Leibler (KL) divergence:*

$$\text{KL} \{p_s(\mathbf{x}|y = 1) || p_t(\mathbf{x}|y = 1)\} < \text{KL} \{p_s(\mathbf{x}|y = 1) || p_t(\mathbf{x}|y = 0)\}.$$

*In the rest of this paper, we assume the DETM is fully identifiable.*

**Remark 2.** *The proposed DETM can be applied to both SCAR and SAR PU data because SCAR data can be viewed as a special case of SAR data with additional constraints. Under*

the SCAR assumption, the distribution of features of positive cases remains the same in the source and target domains. That is

$$\Lambda_1(\mathbf{x}) = \frac{p_t(\mathbf{x}|y=1)}{p_s(\mathbf{x}|y=1)} = 1, \quad (6)$$

for any  $\mathbf{x}$ . We refer to the constrained model for SCAR PU data as the single exponential tilting model (SETM) because we only have the following model assumption:

$$\log \{\Lambda_2(\mathbf{x})\} = \alpha_2 + \mathbf{x}^\top \boldsymbol{\beta}_2.$$

The SETM is a reduced model of DETM because we consider a reduced parameter space where  $\alpha_1 = 0$  and  $\boldsymbol{\beta}_1 = \mathbf{0}$  (implied by (6)). The SETM is similar to the method used in Lancaster and Imbens (1996) in spirit and can also be seen as an extension and refinement of the methods used in Qin (1999) and Qin and Liang (2011) as these methods are constrained to scalar  $x$ .

## 3 Parameter Estimation

### 3.1 Empirical Likelihood Method

Based on the DETM, after combining the source and target data, the log-likelihood function is given by

$$\begin{aligned} \ell &= \sum_{i=1}^n \log \{p_s(\mathbf{x}_i|y=1)\} + \sum_{j=1}^m \log \{p_t(\mathbf{x}_{n+j})\} \\ &= \sum_{i=1}^N \log \{p_s(\mathbf{x}_i|y=1)\} + \sum_{j=1}^m \log \{ \pi \exp(\alpha_1 + \mathbf{x}_{n+j}^\top \boldsymbol{\beta}_1) + (1 - \pi) \exp(\alpha_2 + \mathbf{x}_{n+j}^\top \boldsymbol{\beta}_2) \}, \end{aligned} \quad (7)$$

where  $N \equiv n + m$ . In addition,  $(\alpha_1, \alpha_2, \boldsymbol{\beta}_1, \boldsymbol{\beta}_2)$  and  $p_s(\mathbf{x}|y=1)$  must satisfy the conditions in (5), which can be rewritten as

$$\int \exp(\alpha_1 + \mathbf{x}^\top \boldsymbol{\beta}_1) p_s(\mathbf{x}|y=1) d\mathbf{x} = 1, \quad \int \exp(\alpha_2 + \mathbf{x}^\top \boldsymbol{\beta}_2) p_s(\mathbf{x}|y=1) d\mathbf{x} = 1. \quad (8)$$

The likelihood function (7) is semiparametric because we do not impose any parametric assumption on  $p_s(\mathbf{x}|y = 1)$ . Although the semiparametric likelihood enjoy benefits such as robustness, it also poses significant challenges for parameter estimation. We cannot directly derive the maximum likelihood estimates of  $(\alpha_1, \alpha_2, \boldsymbol{\beta}_1, \boldsymbol{\beta}_2)$  because they are intertwined with the nonparametric density  $p_s(\mathbf{x}|y = 1)$  due to the constraints in (8).

We propose to use the EL method (Owen 1990; Qin and Lawless 1994; Owen 2001) to estimate parameters. The EL method allows us to estimate parameters without assuming a specific distribution assumption on  $p_s(\mathbf{x}|y = 1)$ . Specifically, we denote  $p_i = p_s(\mathbf{x}_i|y = 1)$  for  $i = 1, \dots, N$  and treat them as parameters. Then the log-EL function is given by

$$\begin{aligned} & \ell_{\text{EL}}(\alpha_1, \alpha_2, \boldsymbol{\beta}_1, \boldsymbol{\beta}_2, \pi, p_1, \dots, p_N) \\ &= \sum_{i=1}^N \log(p_i) + \sum_{j=1}^m \log \left\{ \pi \exp(\alpha_1 + \mathbf{x}_{n+j}^T \boldsymbol{\beta}_1) + (1 - \pi) \exp(\alpha_2 + \mathbf{x}_{n+j}^T \boldsymbol{\beta}_2) \right\}. \end{aligned} \quad (9)$$

Note that the feasible values of  $p_i, i = 1, \dots, N$  must satisfy following conditions

$$p_i \geq 0, \quad \sum_{i=1}^N p_i = 1, \quad \sum_{i=1}^N p_i \exp(\alpha_1 + \mathbf{x}_i^T \boldsymbol{\beta}_1) = 1, \quad \sum_{i=1}^N p_i \exp(\alpha_2 + \mathbf{x}_i^T \boldsymbol{\beta}_2) = 1. \quad (10)$$

The first two conditions in (10) are due to the requirement of  $p_s(\mathbf{x}|y = 1)$  being a probability density function; the last two conditions are from (8). Now, the goal is to find out the maximum EL estimator (MELE) of unknown parameters by maximizing the log-EL function in (9).

Let  $\boldsymbol{\theta} = (\alpha_1, \alpha_2, \boldsymbol{\beta}_1, \boldsymbol{\beta}_2, \pi)$ . Using the Lagrange multiplier method, it can be shown that the maximizer of the log-EL function for  $p_i$  given  $\boldsymbol{\theta}$  is

$$p_i = \frac{1}{N} \frac{1}{1 + \sum_{t=1}^2 \lambda_t \{ \exp(\alpha_t + \mathbf{x}_i^T \boldsymbol{\beta}_t) - 1 \}},$$

where the Lagrange multipliers  $(\lambda_1, \lambda_2)$  are solutions to

$$\sum_{i=1}^N \frac{\exp(\alpha_t + \mathbf{x}_i^T \boldsymbol{\beta}_t) - 1}{1 + \sum_{j=1}^2 \lambda_j \{ \exp(\alpha_j + \mathbf{x}_i^T \boldsymbol{\beta}_j) - 1 \}} = 0, \quad t = 1, 2. \quad (11)$$

The profile log-EL function (after maximizing out  $p_i, i = 1, \dots, N$ ) of  $\boldsymbol{\theta}$  is given by

$$\begin{aligned} \ell_N(\boldsymbol{\theta}) = & - \sum_{i=1}^N \log \left[ 1 + \sum_{t=1}^2 \lambda_t \{ \exp(\alpha_t + \mathbf{x}_i^T \boldsymbol{\beta}_t) - 1 \} \right] \\ & + \sum_{j=1}^m \log \{ \pi \exp(\alpha_1 + \mathbf{x}_{n+j}^T \boldsymbol{\beta}_1) + (1 - \pi) \exp(\alpha_2 + \mathbf{x}_{n+j}^T \boldsymbol{\beta}_2) \}. \end{aligned} \quad (12)$$

The MELE of  $\boldsymbol{\theta}$  is then defined as

$$\hat{\boldsymbol{\theta}} = \arg \max_{\boldsymbol{\theta}} \ell_N(\boldsymbol{\theta}).$$

The explicit form of  $\hat{\boldsymbol{\theta}}$  is generally unknown. In the next subsection, we present an EM-algorithm to numerically compute  $\hat{\boldsymbol{\theta}}$ .

## 3.2 Expectation-Maximization algorithm

Due to the absence of target data labels (i.e.,  $\mathcal{Y} = \{y_{n+1}, \dots, y_N\}$ ), we need to deal with the mixture structure in the log-likelihood function (7), which makes the maximization of (12) difficult. The EM algorithm naturally fits into our problem.

If we have access to the latent labels of the target data, the complete log-EL is

$$\begin{aligned} \ell_{\text{EL}}^{\text{C}}(\boldsymbol{\Theta}) = & \sum_{i=1}^N \log(p_i) + \sum_{j=1}^m \{ y_{n+j}(\alpha_1 + \mathbf{x}_{n+j}^T \boldsymbol{\beta}_1) + (1 - y_{n+j})(\alpha_2 + \mathbf{x}_{n+j}^T \boldsymbol{\beta}_2) \} \\ & + \sum_{j=1}^m \{ y_{n+j} \log(\pi) + (1 - y_{n+j}) \log(1 - \pi) \}, \end{aligned}$$

where  $\boldsymbol{\Theta} = (\alpha_1, \alpha_2, \boldsymbol{\beta}_1, \boldsymbol{\beta}_2, \pi, p_1, \dots, p_N)$ . The EM algorithm is based on the complete log-EL.

The core of the EM algorithm is the EM iteration, which contains an E-step and an M-step. We use  $\boldsymbol{\Theta}^{(r-1)}$  to denote the value of  $\boldsymbol{\Theta}$  after  $r - 1$  EM-iterations,  $r = 1, 2, \dots$ . When  $r = 1$ ,  $\boldsymbol{\Theta}^{(0)}$  denotes the initial value of  $\boldsymbol{\Theta}$ .

**E-Step** We need to calculate

$$Q(\Theta|\Theta^{(r-1)}) = \mathbb{E} \left\{ \ell_{\text{EL}}^C(\Theta) | \mathcal{X}, \Theta^{(r-1)} \right\},$$

where  $\mathcal{X} = \{\mathbf{x}_1, \dots, \mathbf{x}_N\}$  denotes the observed features from both source and target, and the expectation is with respect to the conditional distribution of  $\mathcal{Y}$  given  $\mathcal{X}$  and using  $\Theta^{(r-1)}$  for parameters of the conditional distribution. The function  $Q(\Theta|\Theta^{(r-1)})$  can be obtained by replacing the latent  $\mathcal{Y}$  with their conditional expectations

$$\begin{aligned} \omega_{n+j}^{(r)} &= \mathbb{E}_t(y_{n+j} | \mathbf{x}_{n+j}, \Theta^{(r-1)}) \\ &= \frac{\pi^{(r-1)} \exp(\alpha_1^{(r-1)} + \mathbf{x}_{n+j}^T \boldsymbol{\beta}_1^{(r-1)})}{\pi^{(r-1)} \exp(\alpha_1^{(r-1)} + \mathbf{x}_{n+j}^T \boldsymbol{\beta}_1^{(r-1)}) + (1 - \pi^{(r-1)}) \exp(\alpha_2^{(r-1)} + \mathbf{x}_{n+j}^T \boldsymbol{\beta}_2^{(r-1)})}, \end{aligned}$$

for  $j = 1, \dots, m$ . It can be verified that  $Q(\Theta|\Theta^{(r-1)})$  can be rewritten as

$$\begin{aligned} Q(\Theta|\Theta^{(r-1)}) &= \sum_{i=1}^N \log(p_i) + \sum_{j=1}^m \left\{ \omega_{n+j}^{(r)} (\alpha_1 + \mathbf{x}_{n+j}^T \boldsymbol{\beta}_1) + (1 - \omega_{n+j}^{(r)}) (\alpha_2 + \mathbf{x}_{n+j}^T \boldsymbol{\beta}_2) \right\} \\ &\quad + \sum_{j=1}^m \left\{ \omega_{n+j}^{(r)} \log(\pi) + (1 - \omega_{n+j}^{(r)}) \log(1 - \pi) \right\}. \end{aligned}$$

**M-Step** We update  $\Theta$  from  $\Theta^{(r-1)}$  to  $\Theta^{(r)}$  as

$$\Theta^{(r)} = \arg \max_{\Theta} Q(\Theta|\Theta^{(r-1)}) \quad \text{subject to the constraints in (10).}$$

In the supplementary materials, we show that  $\Theta^{(r)}$  can be obtained in the following steps:

Step 1. Update

$$\pi^{(r)} = \frac{1}{m} \sum_{j=1}^m \omega_{n+j}^{(r)}.$$

Step 2. Let

$$\begin{aligned} Q^{(r)}(\alpha_1^*, \alpha_2^*, \boldsymbol{\beta}_1, \boldsymbol{\beta}_2) &= - \sum_{i=1}^N \log \left\{ 1 + \sum_{t=1}^2 \exp(\alpha_t^* + \mathbf{x}_i^T \boldsymbol{\beta}_t) \right\} \\ &\quad + \sum_{j=1}^m \left\{ \omega_{n+j}^{(r)} (\alpha_1^* + \mathbf{x}_{n+j}^T \boldsymbol{\beta}_1) + (1 - \omega_{n+j}^{(r)}) (\alpha_2^* + \mathbf{x}_{n+j}^T \boldsymbol{\beta}_2) \right\}, \end{aligned} \tag{13}$$



where

$$\alpha_1^* = \alpha_1 + \log \left( \frac{\sum_{j=1}^m \omega_{n+j}^{(r)}}{n} \right), \quad \alpha_2^* = \alpha_2 + \log \left( \frac{\sum_{j=1}^m (1 - \omega_{n+j}^{(r)})}{n} \right).$$

We update  $(\alpha_1^*, \alpha_2^*, \boldsymbol{\beta}_1, \boldsymbol{\beta}_2)$  as

$$(\alpha_1^{*(r)}, \alpha_2^{*(r)}, \boldsymbol{\beta}_1^{(r)}, \boldsymbol{\beta}_2^{(r)}) = \arg \max_{\alpha_1^*, \alpha_2^*, \boldsymbol{\beta}_1, \boldsymbol{\beta}_2} Q^{(r)}(\alpha_1^*, \alpha_2^*, \boldsymbol{\beta}_1, \boldsymbol{\beta}_2).$$

This objective function is proportional to a weighted log-likelihood function of a multinomial logistic regression model with three classes. Thus, in practice, we can easily calculate  $(\alpha_1^{*(r)}, \alpha_2^{*(r)}, \boldsymbol{\beta}_1^{(r)}, \boldsymbol{\beta}_2^{(r)})$  by fitting a multinomial logistic regression, which can be done by most software.

Step 3. Update  $\alpha_1$  and  $\alpha_2$  as

$$\alpha_1^{(r)} = \alpha_1^{*(r)} - \log \left( \frac{\sum_{j=1}^m \omega_{n+j}^{(r)}}{n} \right), \quad \alpha_2^{(r)} = \alpha_2^{*(r)} - \log \left( \frac{\sum_{j=1}^m (1 - \omega_{n+j}^{(r)})}{n} \right).$$

Step 4. Update  $p_i$  as

$$p_i^{(r)} = \frac{1}{n \left\{ 1 + \exp(\alpha_1^{*(r)} + \mathbf{x}_i^T \boldsymbol{\beta}_1^{(r)}) + \exp(\alpha_2^{*(r)} + \mathbf{x}_i^T \boldsymbol{\beta}_2^{(r)}) \right\}}, \quad i = 1, \dots, N.$$

Summarizing the above steps leads to Algorithm 1. We call this parameter estimation method the double exponential tilting-empirical likelihood (DET-EL) method.

The following proposition shows that log-EL  $\ell_{\text{EL}}(\boldsymbol{\Theta}) \equiv \ell_{\text{EL}}(\alpha_1, \alpha_2, \boldsymbol{\beta}_1, \boldsymbol{\beta}_2, \pi, p_1, \dots, p_N)$  does not decrease after each iteration.

**Proposition 1.** *With the EM algorithm described above, we have for  $r \geq 2$*

$$\ell_{\text{EL}}(\boldsymbol{\Theta}^{(r)}) \geq \ell_{\text{EL}}(\boldsymbol{\Theta}^{(r-1)}).$$

The proof of Proposition 1 is given in the supplementary materials. We make two remarks about the EM algorithm. First, note that

$$\ell_{\text{EL}}(\boldsymbol{\Theta}) = \sum_{i=1}^n \log(p_i) + \sum_{j=1}^m \log \left\{ \pi p_{n+j} \exp(\alpha_1 + \mathbf{x}_{n+j}^T \boldsymbol{\beta}_1) + (1 - \pi) p_{n+j} \exp(\alpha_2 + \mathbf{x}_{n+j}^T \boldsymbol{\beta}_2) \right\},$$

---

**Algorithm 1:** DET-EL Method for Parameter Estimation

---

**Data:** Source data  $\{\mathbf{x}_i, y_i = 1\}_{i=1}^n$ ; target data  $\{\mathbf{x}_i\}_{i=n+1}^N$ .

**Result:** Estimates of  $\Theta$ .

initialization;

**while** *not converged* **do**

**E-step:** For  $j = 1, \dots, m$ , compute:

$$\omega_{n+j}^{(r)} = \frac{\pi^{(r-1)} \exp(\alpha_1^{(r-1)} + \mathbf{x}_{n+j}^T \boldsymbol{\beta}_1^{(r-1)})}{\pi^{(r-1)} \exp(\alpha_1^{(r-1)} + \mathbf{x}_{n+j}^T \boldsymbol{\beta}_1^{(r-1)}) + (1 - \pi^{(r-1)}) \exp(\alpha_2^{(r-1)} + \mathbf{x}_{n+j}^T \boldsymbol{\beta}_2^{(r-1)})}.$$

**M-step:**

1. Update  $\pi$  by  $\pi^{(r)} = m^{-1} \sum_{j=1}^m \omega_{n+j}^{(r)}$ ;
2. Update  $(\alpha_1^*, \alpha_2^*, \boldsymbol{\beta}_1, \boldsymbol{\beta}_2)$  by

$$(\alpha_1^{*(r)}, \alpha_2^{*(r)}, \boldsymbol{\beta}_1^{(r)}, \boldsymbol{\beta}_2^{(r)}) = \arg \max_{\alpha_1^*, \alpha_2^*, \boldsymbol{\beta}_1, \boldsymbol{\beta}_2} Q^{(r)}(\alpha_1^*, \alpha_2^*, \boldsymbol{\beta}_1, \boldsymbol{\beta}_2),$$

where  $Q^{(r)}(\alpha_1^*, \alpha_2^*, \boldsymbol{\beta}_1, \boldsymbol{\beta}_2)$  is given in (13);

3. Update  $\alpha_1$  and  $\alpha_2$  by

$$\alpha_1^{(r)} = \alpha_1^{*(r)} - \log \left( \frac{\sum_{j=1}^m \omega_{n+j}^{(r)}}{n} \right), \quad \alpha_2^{(r)} = \alpha_2^{*(r)} - \log \left( \frac{\sum_{j=1}^m (1 - \omega_{n+j}^{(r)})}{n} \right);$$

4. For  $i = 1, \dots, N$ , update  $p_i$ 's by

$$p_i^{(r)} = n^{-1} \left\{ 1 + \exp(\alpha_1^{*(r)} + \mathbf{x}_i^T \boldsymbol{\beta}_1^{(r)}) + \exp(\alpha_2^{*(r)} + \mathbf{x}_i^T \boldsymbol{\beta}_2^{(r)}) \right\}^{-1}.$$

**end**

Determine label switching and output the estimates.

---

which, together with (10), implies that  $\ell_{\text{EL}}(\Theta) \leq 0$ . With this result, Proposition 1 guarantees that the EM algorithm eventually converges to at least a local maximum for the given

initial value  $\Theta^{(0)}$ . We recommend using multiple initial values to explore the likelihood function to ensure achieving the global maximum. Second, in practice, we may stop the algorithm when the increment in the log-EL after an iteration is no greater than, say,  $1e-6$ .

## 4 Theoretical Results

### 4.1 Statistical Inference

In this section, we first provide the asymptotic distribution of the MELE  $\hat{\theta}$ . Then, we focus on two specific statistical inference tasks: the first one is the goodness-of-fit test of the SETM as opposed to the DETM; the second one is inference on the mixture proportion  $\pi$ .

We need some notation for developing the asymptotic distribution for  $\hat{\theta}$ . Let  $(\hat{\lambda}_1, \hat{\lambda}_2)$  be the Lagrange multipliers corresponding to  $\hat{\theta}$ , i.e.,  $(\hat{\lambda}_1, \hat{\lambda}_2)$  is the solution of (11) with  $\theta$  being replaced by  $\hat{\theta}$ . Throughout the paper, we assume that the total sample size  $N = n+m \rightarrow \infty$  and  $m/N \rightarrow c$  for some constant  $c \in (0, 1)$ . This assumption indicates that  $n$  and  $m$  go to infinity at the same rate. For simplicity and presentation convenience, we write  $c = m/N$  and assume it is a constant, which does not affect our technical development. The following theorem establishes the joint asymptotic normality of  $(\hat{\lambda}_1, \hat{\lambda}_2)$  and  $\hat{\theta}$ , which implies the asymptotic normality of  $\hat{\theta}$ . The proofs for results in this section will be given in the supplementary materials.

**Theorem 2.** *Suppose the DETM and regularity conditions in Appendix are satisfied. Let  $\theta^o = (\alpha_1^o, \alpha_2^o, \beta_1^o, \beta_2^o, \pi^o)$  be the true value of  $\theta$ . As  $N$  goes to infinity,*

$$\sqrt{N} \left\{ \hat{\lambda}_1 - c\pi^o, \hat{\lambda}_2 - c(1 - \pi^o), (\hat{\theta} - \theta^o)^T \right\}^T \rightarrow N(\mathbf{0}, \Sigma)$$

*in distribution, where  $\Sigma$  is given in (16) in Appendix.*

For SCAR PU data, using the DETM might not be the best approach as SETM could improve computational and estimation efficiency in such cases. To help us decide whether the SETM can provide a good fit to the PU data, we can use the profile log-EL function in (12) to construct the goodness-of-fit test of the SETM as opposed to the DETM. Specifically, the empirical likelihood ratio (ELR) test for testing SETM vs. DETM can be formulated as the following null hypothesis  $H_0 : \alpha_1 = 0$  and  $\beta_1 = \mathbf{0}$  with test statistic given by

$$R_N = 2 \left\{ \ell_N(\widehat{\boldsymbol{\theta}}) - \ell_N(\widetilde{\boldsymbol{\theta}}) \right\},$$

where  $\widetilde{\boldsymbol{\theta}}$  is the MELE of  $\boldsymbol{\theta}$  under the SETM with  $\alpha_1 = 0$  and  $\beta_1 = \mathbf{0}$ , and  $\widehat{\boldsymbol{\theta}}$  is the MELE under the DETM. Note that  $\widetilde{\boldsymbol{\theta}}$  can be obtained by slightly modifying Algorithm 1: we only need to fix  $\alpha_1 = 0$  and  $\beta_1 = \mathbf{0}$  in the E-step and M-step of Algorithm 1.

For the inference of  $\pi$ , the profile log-EL function in (12) can also be used to define the ELR function of  $\pi$  as

$$R_N^*(\pi) = 2 \left\{ \ell_N(\widehat{\boldsymbol{\theta}}) - \ell_N(\widehat{\boldsymbol{\theta}}_\pi) \right\},$$

where  $\widehat{\boldsymbol{\theta}}_\pi$  is the MELE of  $\boldsymbol{\theta}$  with  $\pi$  being fixed. We can derive  $\widehat{\boldsymbol{\theta}}_\pi$  as if we know the value of  $\pi$  in Algorithm 1: we only need to fix  $\pi$  in the E-step and M-step of Algorithm 1.

Let  $\pi^o$  be the true value of  $\pi$  with  $0 < \pi^o < 1$ . The following theorem summarizes the asymptotic results of  $R_N$  and  $R_N^*(\pi^o)$ .

**Theorem 3.** *Assume the same conditions as Theorem 2. We have*

(a)  $R_N \xrightarrow{d} \chi_p^2$  as  $N \rightarrow \infty$  under the null hypothesis  $H_0 : \alpha_1 = 0$  and  $\beta_1 = \mathbf{0}$ , where  $p$  is the dimension of  $\beta_1$ .

(b)  $R_N^*(\pi^o) \xrightarrow{d} \chi_1^2$  as  $N \rightarrow \infty$ .

Based on Theorem 3, we can perform hypothesis tests for  $\pi$  and the goodness-of-fit of the SETM on the PU data. For example, we can reject the SETM and adopt the DETM at significant level 0.05 if  $R_N > \chi_{p,0.95}^2$ , where  $\chi_{p,0.95}^2$  is the 95% quantile of  $\chi_p^2$ . In addition, we can also construct the ELR-based confidence interval for the mixture proportion  $\pi$ . For example, a 95% confidence interval for  $\pi$  is given by  $\{\pi : R_N^*(\pi) \leq \chi_{1,0.95}^2\}$ .

## 4.2 Approximation of the Bayes Classifier

Recall that the Bayes classifier in Section 2.1 depends on  $\Pr_t(Y = 1|\mathbf{X} = \mathbf{x})$  in (2). Under the DETM in (4),  $\Pr_t(Y = 1|\mathbf{X} = \mathbf{x})$  can be rewritten as

$$\phi(\mathbf{x}; \boldsymbol{\theta}) \equiv \Pr_t(Y = 1|\mathbf{X} = \mathbf{x}) = \frac{\pi \exp(\alpha_1 + \mathbf{x}^T \boldsymbol{\beta}_1)}{\pi \exp(\alpha_1 + \mathbf{x}^T \boldsymbol{\beta}_1) + (1 - \pi) \exp(\alpha_2 + \mathbf{x}^T \boldsymbol{\beta}_2)}.$$

With the MELE of  $\boldsymbol{\theta}$ , we estimate  $\Pr_t(Y = 1|\mathbf{X} = \mathbf{x})$  by  $\phi(\mathbf{x}; \hat{\boldsymbol{\theta}})$ , thus approximating the Bayes classifier. In the following theorem, we show that the  $L_1$ -distance between  $\phi(\mathbf{x}; \hat{\boldsymbol{\theta}})$  and  $\phi(\mathbf{x}; \boldsymbol{\theta}^o)$  has the order  $N^{-1/2}$ .

**Theorem 4.** *Assume the same conditions as Theorem 2. We have*

$$\int \left| \phi(\mathbf{x}; \hat{\boldsymbol{\theta}}) - \phi(\mathbf{x}; \boldsymbol{\theta}^o) \right| p_t(\mathbf{x}) d\mathbf{x} = O_p(N^{-1/2}).$$

## 5 Numerical Studies

In this section, we first present an ablation study to evaluate the proposed method. Then, we apply our method to a real data application to predict the selling price of mobile phones. We conducted the numerical study on a MacBook with an M3 Pro chip and 36 GB of RAM, using R version 4.4.0 (R Core Team, 2024), and our custom package PUEM given in the supplementary materials. Some benchmark methods were implemented in Python version 3.11.7 because the authors only provide Python source code.

## 5.1 Ablation Study

We conduct an ablation study to assess the performance of our proposed framework across various tasks. We are interested in the following tasks: 1) Conducting a goodness-of-fit test between SETM and DETM, focusing on the type-I error and power of the test procedure. 2) Evaluating the mean square error (MSE) of the MELE of  $\pi$ . 3) Determining the coverage accuracy of the confidence intervals of  $\pi$ . 4) Assessing the classification accuracy using the approximated Bayes classifier.

**Detection of SCAR Data** Letting  $\mathbf{0}_p$  and  $\mathbf{1}_p$  column vectors of 0’s and 1’s with dimension  $p$ , respectively, we generated data with the following multivariate normal distributions: 1) Source positive distribution:  $p_s(\mathbf{x}|y = 1) \sim \text{MVN}(\boldsymbol{\mu}_1, \mathbf{I})$ , where  $\boldsymbol{\mu}_1 = \mathbf{0}_{15} \in \mathbf{R}^{15}$ . 2) Target negative distribution:  $p_t(\mathbf{x}|y = 0) \sim \text{MVN}(\boldsymbol{\mu}_2, \mathbf{I})$ , where  $\boldsymbol{\mu}_2 = \mathbf{1}_{15} \in \mathbf{R}^{15}$ . 3) Target positive distribution:  $p_t(\mathbf{x}|y = 1) \sim \text{MVN}(\boldsymbol{\mu}_3, \mathbf{I})$ , where we can choose different levels for  $\boldsymbol{\mu}_3$ :  $\boldsymbol{\mu}_3 \in \{\mathbf{0}_{15}, (1 \ \mathbf{0}_{14}^T)^T, \dots, (\mathbf{1}_7^T \ \mathbf{0}_8^T)^T\}$ . We shall note that when  $\boldsymbol{\mu}_3 = \mathbf{0}_{15}$ , the PU data are SCAR; otherwise, the data are SAR. We performed the goodness-of-fit test for SETM vs. DETM, where the null hypothesis is that the PU data are SCAR and follow the SETM, which can be translated to  $H_0 : \alpha_1 = 0$  and  $\boldsymbol{\beta}_1 = \mathbf{0}_{15}$ .

In the experiment, we set the sample size of the source data equal to that of the target data ( $n = m$ ) and fixed the proportion of positive data on the target at 75% ( $\pi = 0.75$ ). The levels of  $n$  were 1000, 2000, 3000, 4000, and 5000. Each factor level combination was repeated 500 times. Table 1 summarizes the rejection rates of the goodness-of-fit test at the 5% significance level.

When  $\boldsymbol{\mu}_1 = \boldsymbol{\mu}_3 = \mathbf{0}_{15}$  (i.e., the null hypothesis is true; see column “0”), the rejection rate (i.e., the type-I error) converges to the nominal significant value 0.05 as sample size  $n$  increases, which honors the asymptotic results in Section 4.1. For columns “1” through “7”,

Table 1: Rejection rates of the goodness-of-fit test for testing  $H_0 : \alpha_1 = 0$  and  $\beta_1 = \mathbf{0}_{15}$ .

$n$	Number of “1”s in $\boldsymbol{\mu}_3$							
	0	1	2	3	4	5	6	7
1000	11.0%	100%	100%	100%	100%	100%	100%	99.8%
2000	9.2%	100%	100%	100%	100%	100%	100%	100%
3000	7.8%	100%	100%	100%	100%	100%	100%	100%
4000	5.4%	100%	100%	100%	100%	100%	100%	100%
5000	5.4%	100%	100%	100%	100%	100%	100%	100%

the null hypothesis does not hold because  $\boldsymbol{\mu}_3 \neq \boldsymbol{\mu}_1$ , and the rejection rates (i.e., power) are nearly uniformly 100%, indicating that the proposed hypothesis test almost always rejects the null, even if  $\boldsymbol{\mu}_3$  and  $\boldsymbol{\mu}_1$  differ in only one dimension.

**Estimations and Confidence Intervals for the Mixture Proportion** We used two different data-generating mechanisms in this task. The first one generates SCAR PU data, where the source positive (i.e.,  $p_s(\mathbf{x}|y = 1)$ ) and target positive (i.e.,  $p_t(\mathbf{x}|y = 1)$ ) distributions are the same and are set as  $\text{MVN}(\mathbf{0}_{15}, \mathbf{I})$ ; whereas the target negative distribution is set as  $p_t(\mathbf{x}|y = 0) \sim \text{MVN}(\mathbf{1}_{15}, \mathbf{I})$ . The second one generates SAR PU data, where the source positive distribution is set as  $\text{MVN}(\mathbf{0}_{15}, \mathbf{I})$ , the target positive distribution is set as  $\text{MVN}((\mathbf{1}_7^T \ \mathbf{0}_8^T)^T, \mathbf{I})$ , and the target negative distribution is  $\text{MVN}(\mathbf{1}_{15}, \mathbf{I})$ .

Similar to the previous task, we let  $n = m$  and varied  $n$  in  $\{1000, 2000, 3000, 4000, 5000\}$ . We experimented on two values of  $\pi \in \{0.3, 0.7\}$  and repeated each factor level combination for 500 times. We estimated the mixture proportion  $\pi = \text{Pr}_t(Y = 1)$  and constructed confidence intervals for every replicate of each factor level combination using both the DETM and SETM.

The estimation results are summarized in Table 2 and Figure 2. In the case of the SCAR PU data, both the DETM and SETM provide good estimates. In the left panel of Table 2, we see that the estimated bias, standard deviation, and MSE are all small. Regarding the estimation efficiency, illustrated in the first row of Figure 2, we observe that the SETM outperforms DETM, albeit marginally. The efficiency gain is due to that the SETM is a reduced model of DETM. For the SAR data, the DETM method still performed well with MSE shrinking toward 0 as the sample size increases. However, the SETM failed due to model misspecification as illustrated in the second row of Figure 2 and the right panel of Table 2.

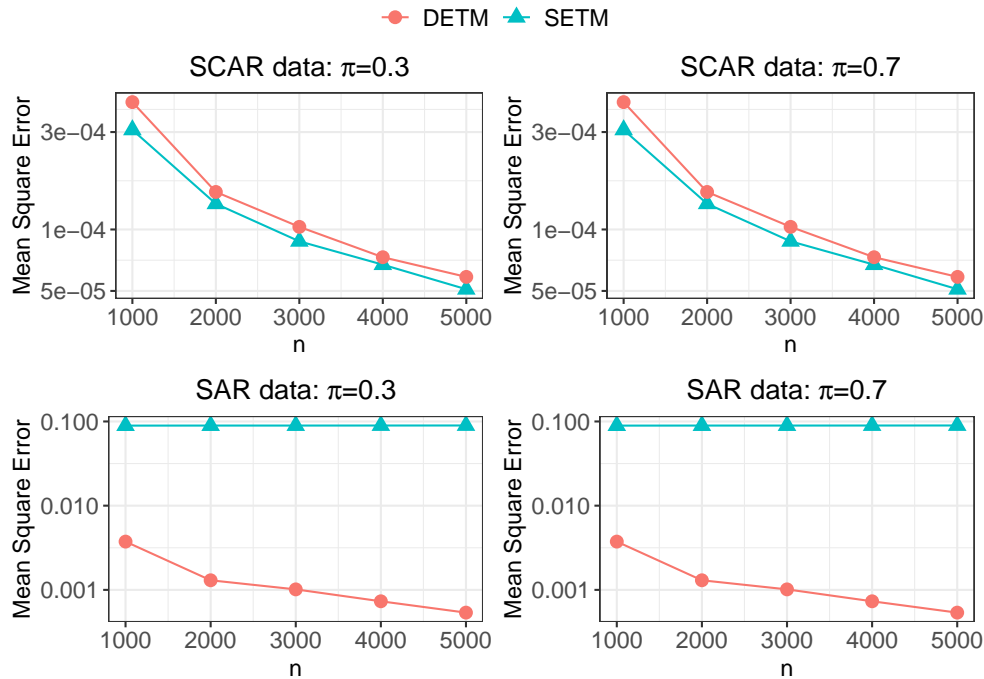


Figure 2: MSE of  $\pi$  estimates.

We also constructed two-sided 95% confidence intervals for  $\pi$ , and the results are given in Figure 3. We report the estimated coverage probabilities in each of the different scenarios: 1) SETM on the SCAR PU data, 2) DETM on the SCAR PU data, 3) SETM on the SAR PU data, and 4) DETM on the SAR PU data. For the SCAR data, the coverage



Table 2: The estimated means and standard deviations (in parenthesis) of  $\pi$  estimates.

$n$	SCAR Data				SAR Data			
	SETM		DETM		SETM		DETM	
	$\pi = 0.3$	$\pi = 0.7$	$\pi = 0.3$	$\pi = 0.7$	$\pi = 0.3$	$\pi = 0.7$	$\pi = 0.3$	$\pi = 0.7$
1000	0.301 (0.018)	0.702 (0.020)	0.302 (0.020)	0.700 (0.023)	0.001 (0.002)	0.999 (0.002)	0.307 (0.061)	0.669 (0.064)
2000	0.300 (0.012)	0.699 (0.014)	0.300 (0.012)	0.700 (0.015)	0.001 (0.001)	0.999 (0.001)	0.304 (0.036)	0.688 (0.047)
3000	0.300 (0.009)	0.700 (0.011)	0.300 (0.010)	0.700 (0.012)	0.001 (0.001)	1.000 (0.001)	0.304 (0.032)	0.697 (0.040)
4000	0.300 (0.008)	0.699 (0.009)	0.300 (0.009)	0.699 (0.010)	0.001 (0.001)	1.000 (0.001)	0.302 (0.027)	0.694 (0.033)
5000	0.300 (0.007)	0.699 (0.008)	0.300 (0.008)	0.699 (0.008)	0.001 (0.001)	1.000 (0.001)	0.302 (0.023)	0.694 (0.029)

probabilities of both DETM and SETM reach the nominal level of 95% as the sample size increases. However, when the data are SAR, the confidence intervals constructed using the SETM fail to cover the true parameter value  $\pi$ , resulting in a coverage probability that is close to 0. On the other hand, the DETM's confidence intervals still perform well, remaining around the nominal levels of 95%.

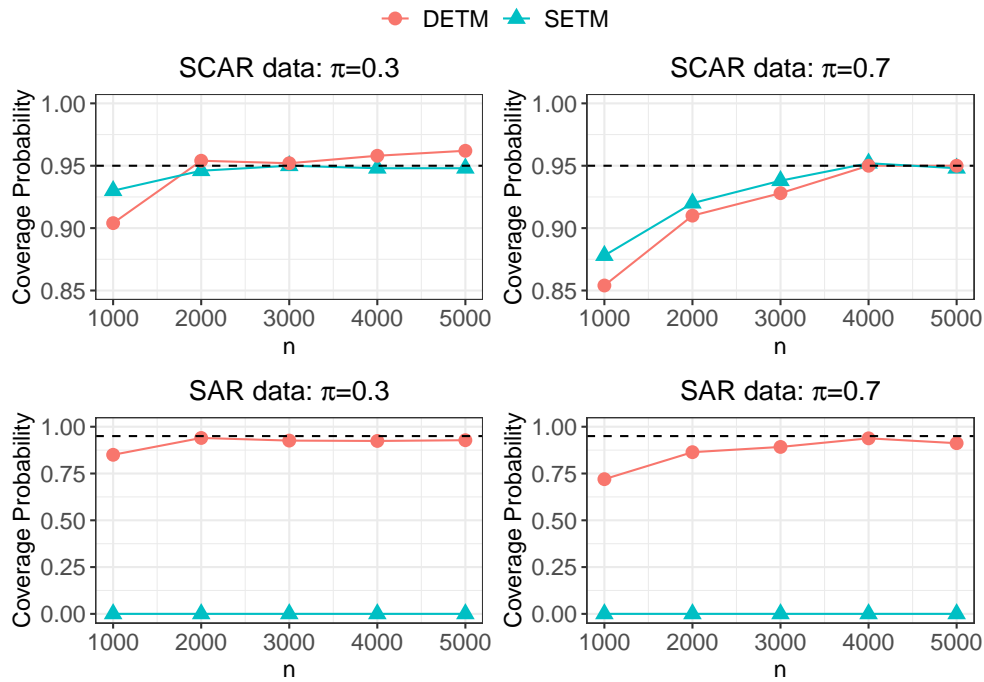


Figure 3: Coverage probabilities of confidence intervals for  $\pi$ .

**Classification Accuracy** Lastly, we aim to assess the prediction performance of our proposed method. We generate the SCAR and SAR data the same way as in the “Estimations and Confidence Intervals for the Mixture Proportion” part, where  $\pi \in \{0.3, 0.7\}$  and  $n = m \in \{1000, 2000, 3000, 4000, 5000\}$ . To avoid overfitting, we generate a new validation dataset from the target distribution  $p_t(\mathbf{x}, y)$  with sample size  $n$ , and the classifiers are applied to the validation dataset to calculate the classification accuracy.

We compare the following methods, including ours and some existing methods in the machine learning literature. 1) DETM: the proposed approximated Bayes classifier by replacing parameters with the MELEs under the DETM. 2) SETM: the approximated Bayes classifier by replacing parameters with the MELEs under the SETM. 3) PS: proposed by Bekker et al. (2019) and is based on the propensity score function. 4) KM2: proposed by Ramaswamy et al. (2016) using the reproducing kernel Hilbert space and is based on SCAR PU data. 5) TICE: proposed by Bekker and Davis (2018) and is based on SCAR PU data.

Figure 4 illustrates the classification accuracies using 100 replicates. When the data are SCAR and  $\pi = 0.3$ , all classifiers performed well, achieving an accuracy exceeding 95% across all sample sizes. However, when  $\pi = 0.7$ , the KM2 method had the lowest accuracy at around 87%, while all other methods maintained at least 90% accuracy across all sample sizes.

For the SAR data, the simulation studies highlight discrepancies among different methods. In both  $\pi = 0.3$  and  $\pi = 0.7$  scenarios, our proposed DETM method achieves the highest classification rate of around 90%, with accuracy improving as the sample size increases. In comparison, at  $\pi = 0.3$ , all benchmark methods have accuracies between 70% and 80%, with SETM performing the worst across all sample sizes. When  $\pi = 0.7$ , the

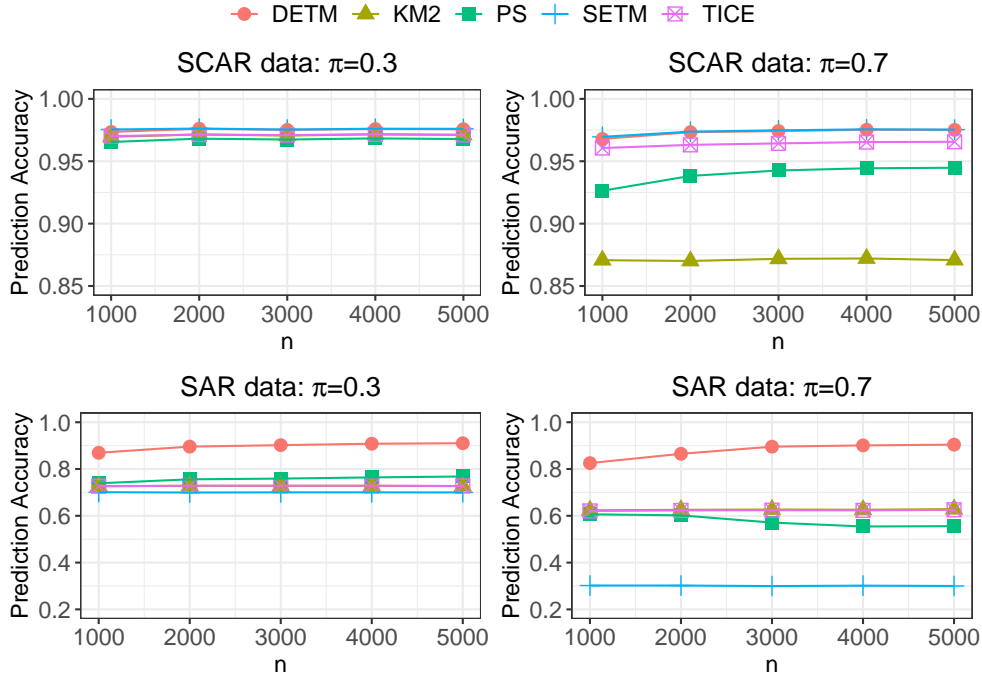


Figure 4: Classification accuracies of five classifiers.

accuracies of benchmark methods PS, KM2, and TICE are around 60%. SETM again has the worst performance.

**Summary** The ablation study demonstrates that our proposed DETM method excels in estimation, inference, and classification tasks, regardless of whether SAR or SCAR data are used. Under correct model assumptions, the SETM method performs well, with slightly improved estimation efficiency compared to DETM. However, SETM lacks robustness and performs poorly across all tasks when the SCAR assumption is violated. Additionally, the goodness-of-fit test effectively distinguishes SAR data by accurately identifying SCAR data with a type-I error rate close to the nominal level and exhibiting high power in detecting non-SCAR data. For classification tasks, the proposed DETM method also shows superior performance compared to existing methods.

## 5.2 Mobile Phone Dataset

This section demonstrates the proposed methodology using a real data application. We consider the Mobile Phone Dataset from the Kaggle <sup>1</sup>. The Mobile Phone Dataset contains 20 features and an ordinal label taking values in the set  $\{0, 1, 2, 3\}$  that indicates the phone’s price range from low cost to very high cost. Under each class, there are 500 observations. The features include properties such as the memory size and the phone’s weight; see Table S1 in the supplementary materials for the full list of the features.

Before the analysis, we first preprocess the dataset to fit our needs. We first merge classes 0 and 1 to form the positive target data from  $p_t(\mathbf{x}|y = 1)$  (low-end phone). We then use class 2 as the positive source data from  $p_s(\mathbf{x}|y = 1)$  (low-end phone) and class 3 as negative target data from  $p_t(\mathbf{x}|y = 0)$  (high-end phone). Then, the source positive data have a sample size of  $n = 500$ , and the target data have a sample size of  $m = 1500$ , where 500 are positive and 1000 are negative. Our formulation ensures that the low-end phones in the source and target are different, as low-end phones in the target data are less expensive; thus, the data can be seen as SAR PU.

We first conducted the goodness-of-fit test for SETM vs. DETM. The value of the ELR statistic is  $R_N = 1218.628$ , which gives a p-value of 0, calibrated by the limiting distribution  $\chi_{20}^2$ . Hence, we reject the null hypothesis with overwhelming evidence and adopt the DETM. The test results also align with the way we construct the PU data. Next, we examine the estimation and inference of the mixture proportion  $\pi$ . The true  $\pi$  in the target data is  $\pi_0 = n_1/(n_1 + n_3) = 2/3$ , and the estimate  $\hat{\pi} = 0.667$  is close to the true value. For the inference of  $\pi$ , we examine the behavior of the ELR function  $R_N^*(\pi)$  in Figure 5. The vertical solid blue line is the true value of  $\pi$ . The red horizontal line is the

---

<sup>1</sup>Available at <https://www.kaggle.com/datasets/iabhishekofficial/mobile-price-classification>

95% quantile of  $\chi_1^2$ , and the two dashed lines indicate the two endpoints of a 95% confidence interval. We can see that the true value is within the confidence interval  $[0.6425, 0.6903]$ .

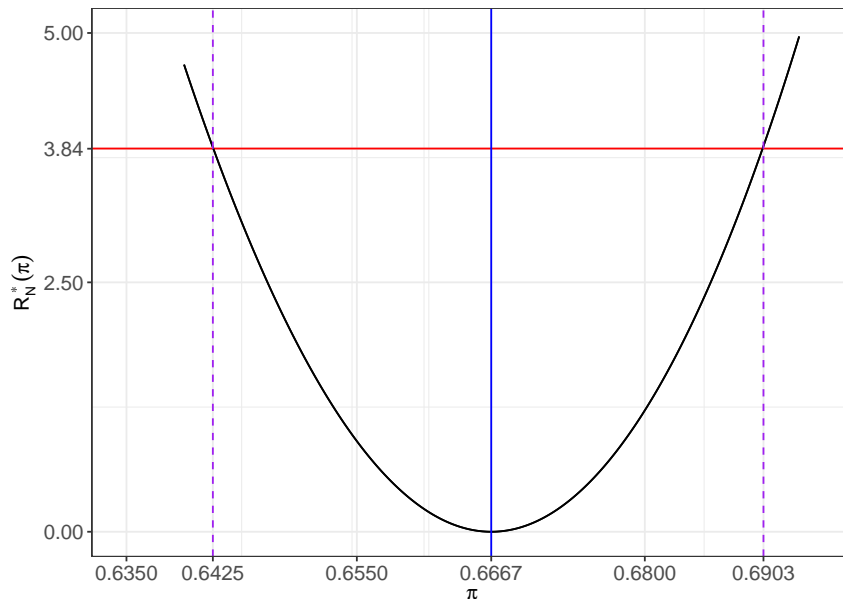


Figure 5: Plot of the ELR function  $R_N^*(\pi)$  versus  $\pi$ .

Lastly, we focus on the classification. Letting the sample size of the positive target, positive source, and negative target data be  $n_1 = 1000, n_2 = 500$ , and  $n_3 = 500$ , respectively, we reserve 20% of the positive target and negative target data and combine them for verification to avoid overfitting. Thus, the PU data have a sample size of  $N = n + m$ , where  $n = n_2 = 500$  and  $m = 0.8n_1 + 0.8n_3 = 1200$ . The sample size of the verification dataset is  $0.2n_1 + 0.2n_3$ . We repeated the data partition on the target data for 20 times and performed classification for each replicate. We compared the proposed DETM method with the benchmarks used in the ablation study. Table 3 summarizes the average classification accuracy from 20 sample splitting replicates. The numbers in the parenthesis are the standard deviation of the 20 accuracies from 20 replicates. Our proposed method, DETM, has surprisingly achieved perfect classification, whereas the benchmark methods have accuracies around 89.15% to 91.23%.

Table 3: Classification accuracies on the Mobile Phone Dataset.

Method	DETM	PS	KM2	TICE
Accuracy	100% (0%)	91.23% (1.2%)	89.15% (3.23%)	88.42% (1.78%)

## 6 Concluding Remarks

We conclude by highlighting several promising directions for future research. One intriguing extension involves exploring the open set label shift setting (e.g., Garg et al. 2022), where the target domain introduces a new class not present in the source domain, but the source domain has multiple classes. This setting expands the scope of PU data and presents new challenges and opportunities for DETM to demonstrate its adaptability and effectiveness. Another critical area for future investigation is the robustness of DETM in the presence of noisy labels. Enhancing the model’s resilience to such imperfections is vital for ensuring reliable performance in real-world applications, where data quality can often be compromised.

## Appendix: Form of $\Sigma$ and Regularity Conditions

We note that the log-EL function in (12) can be rewritten as  $\ell_N(\boldsymbol{\theta}) = \min_{\lambda_1, \lambda_2} h(\lambda_1, \lambda_2, \boldsymbol{\theta})$ , where

$$\begin{aligned}
 h(\lambda_1, \lambda_2, \boldsymbol{\theta}) = & - \sum_{i=1}^N \log \left[ 1 + \sum_{t=1}^2 \lambda_t \{ \exp(\alpha_t + \mathbf{x}_i^T \boldsymbol{\beta}_t) - 1 \} \right] \\
 & + \sum_{j=1}^m \log \{ \pi \exp(\alpha_1 + \mathbf{x}_{n+j}^T \boldsymbol{\beta}_1) + (1 - \pi) \exp(\alpha_2 + \mathbf{x}_{n+j}^T \boldsymbol{\beta}_2) \}. \quad (14)
 \end{aligned}$$

Equivalently,  $\ell_N(\boldsymbol{\theta}) = h(\lambda_1, \lambda_2, \boldsymbol{\theta})$  with  $(\lambda_1, \lambda_2)$  being the solution to  $\partial h(\lambda_1, \lambda_2, \boldsymbol{\theta}) / \partial \lambda_1 = 0$  and  $\partial h(\lambda_1, \lambda_2, \boldsymbol{\theta}) / \partial \lambda_2 = 0$ .

The form of  $\Sigma$  depends on the first and second derivatives of  $h(\lambda_1, \lambda_2, \boldsymbol{\theta})$  with respect

to  $\lambda_1$ ,  $\lambda_2$ , and  $\boldsymbol{\theta}$ . Specifically, let  $\mathbf{v} = (\lambda_1, \lambda_2, \boldsymbol{\theta}^\top)^\top$ ,  $\mathbf{v}^o = (c\pi^o, c(1 - \pi^o), \boldsymbol{\theta}^{o\top})^\top$ , and  $h(\mathbf{v}) = h(\lambda_1, \lambda_2, \boldsymbol{\theta})$ . Further, let

$$\mathbf{V} = N^{-1}\mathbb{E}\left\{\frac{\partial h(\mathbf{v}^o)}{\partial \mathbf{v}}\frac{\partial h(\mathbf{v}^o)}{\partial \mathbf{v}^\top}\right\} \quad \text{and} \quad \mathbf{W} = -N^{-1}\mathbb{E}\left\{\frac{\partial^2 h(\mathbf{v}^o)}{\partial \mathbf{v}\partial \mathbf{v}^\top}\right\}. \quad (15)$$

It can be verified that both  $\mathbf{V}$  and  $\mathbf{W}$  are independent of the total sample size  $N$ . The detailed forms of  $\mathbf{V}$  and  $\mathbf{W}$  are given in the supplementary materials. The matrix  $\boldsymbol{\Sigma}$  is then defined as

$$\boldsymbol{\Sigma} = \mathbf{W}^{-1}\mathbf{V}\mathbf{W}^{-1}. \quad (16)$$

The asymptotic results in Section 4 rely on the following regularity conditions. Let  $\mathbf{q}(\mathbf{x}) = (1, \mathbf{x}^\top)^\top$  and  $\mathbb{E}_s$  denote the expectation with respect to  $p_s(\mathbf{x}|y = 1)$ .

C1. The total sample size  $N = n + m \rightarrow \infty$  and  $m/N \rightarrow c$  for some constant  $c \in (0, 1)$ .

Furthermore,  $0 < \pi^o < 1$ , and  $\boldsymbol{\theta}^o$  is an interior point of the parameter space for  $\boldsymbol{\theta}$ .

C2. The function  $\mathbb{E}_s\{\exp(\mathbf{X}^\top\boldsymbol{\beta})\}$  is finite when  $\boldsymbol{\beta}$  is in a small neighborhood of  $\boldsymbol{\beta}_1^o$  and  $\boldsymbol{\beta}_2^o$ .

C3.  $\mathbb{E}_s\{\mathbf{q}(\mathbf{X})\mathbf{q}(\mathbf{X})^\top\}$  exists and is positive definite.

C4.  $\mathbf{W}$  has the full rank.

As we commented before, Condition C1 indicates that both  $n$  and  $m$  go to infinity at the same rate. Condition C2 guarantees the existence of finite moments of  $\mathbf{q}(\mathbf{X})$  under  $p_s(\mathbf{x}|y = 1)$ ,  $p_t(\mathbf{x}|y = 0)$ , and  $p_t(\mathbf{x}|y = 1)$ . Condition C3 is an identifiability condition, and it ensures that the components of  $\mathbf{q}(\mathbf{x})$  are linearly independent under  $p_s(\mathbf{x}|y = 1)$ ,  $p_t(\mathbf{x}|y = 0)$ , and  $p_t(\mathbf{x}|y = 1)$ . Hence, the elements of  $\mathbf{q}(\mathbf{x})$  except the first cannot be constant functions. Conditions C1–C4 guarantee that quadratic approximations of the profile log-EL function  $\ell_N(\boldsymbol{\theta})$  are applicable.

## References

- Begg, C. B. (1994). Methodological issues in studies of the treatment, diagnosis, and etiology of prostate cancer. *Seminars in Oncology*, 21.
- Bekker, J. and Davis, J. (2018). Estimating the class prior in positive and unlabeled data through decision tree induction. In *AAAI Conference on Artificial Intelligence*.
- Bekker, J. and Davis, J. (2020). Learning from positive and unlabeled data: a survey. *Machine Learning*, 109.
- Bekker, J., Robberechts, P., and Davis, J. (2019). Beyond the selected completely at random assumption for learning from positive and unlabeled data. In *European Conference on Machine Learning and Principles and Practice of Knowledge Discovery in Databases*.
- Coudray, O., Keribin, C., Massart, P., and Pamphile, P. (2023). Risk bounds for positive-unlabeled learning under the selected at random assumption. *Journal of Machine Learning Research*, 24.
- Duan, R., Ning, Y., Wang, S., Lindsay, B. G., Carroll, R. J., and Chen, Y. (2020). A fast score test for generalized mixture models. *Biometrics*, 76.
- Elkan, C. and Noto, K. (2008). Learning classifiers from only positive and unlabeled data. In *ACM SIGKDD International Conference on Knowledge Discovery and Data Mining*.
- Furmańczyk, K., Mielniczuk, J., Rejchel, W., and Teisseyre, P. (2022). Joint estimation of posterior probability and propensity score function for positive and unlabelled data. *arXiv:2209.07787*.
- Garg, S., Balakrishnan, S., and Lipton, Z. (2022). Domain adaptation under open set label shift. In *Advances in Neural Information Processing Systems*.



- Garg, S., Wu, Y., Smola, A. J., Balakrishnan, S., and Lipton, Z. (2021). Mixture proportion estimation and PU learning: a modern approach. In *Advances in Neural Information Processing Systems*.
- Godley, P. A. and Schell, M. J. (1999). Adjusted odds ratios under nondifferential misclassification: application to prostate cancer. *Journal of Clinical Epidemiology*, 52.
- Gong, C., Wang, Q., Liu, T., Han, B., You, J. J., Yang, J., and Tao, D. (2021). Instance-dependent positive and unlabeled learning with labeling bias estimation. *IEEE Transactions on Pattern Analysis and Machine Intelligence*.
- Jaskie, K. and Spanias, A. (2019). Positive and unlabeled learning algorithms and applications: A survey. In *International Conference on Information, Intelligence, Systems and Applications*.
- Kato, M., Teshima, T., and Honda, J. (2019). Learning from positive and unlabeled data with a selection bias. In *International Conference on Learning Representations*.
- Kim, H., Zhang, X., Zhao, J., and Tian, Q. (2024). ReTaSA: A nonparametric functional estimation approach for addressing continuous target shift. In *International Conference on Learning Representations*.
- Lancaster, T. and Imbens, G. (1996). Case-control studies with contaminated controls. *Journal of Econometrics*, 71.
- Lipton, Z., Wang, Y.-X., and Smola, A. (2018). Detecting and correcting for label shift with black box predictors. In *International Conference on Machine Learning*.
- Maity, S., Yurochkin, M., Banerjee, M., and Sun, Y. (2023). Understanding new tasks

- through the lens of training data via exponential tilting. In *International Conference on Learning Representations*.
- Owen, A. (1990). Empirical likelihood ratio confidence regions. *The Annals of Statistics*, 18.
- Owen, A. (2001). *Empirical Likelihood*. CRC Press.
- Qin, J. (1998). Inferences for case-control and semiparametric two-sample density ratio models. *Biometrika*, 85.
- Qin, J. (1999). Empirical likelihood ratio based confidence intervals for mixture proportions. *The Annals of Statistics*, 27.
- Qin, J. (2017). *Biased Sampling, Over-identified Parameter Problems and Beyond*. Springer.
- Qin, J. and Lawless, J. (1994). Empirical likelihood and general estimating equations. *The Annals of Statistics*, 22.
- Qin, J. and Liang, K.-Y. (2011). Hypothesis testing in a mixture case-control model. *Biometrics*, 67.
- R Core Team (2024). *R: A Language and Environment for Statistical Computing*. R Foundation for Statistical Computing.
- Ramaswamy, H., Scott, C., and Tewari, A. (2016). Mixture proportion estimation via kernel embeddings of distributions. In *International Conference on Machine Learning*.
- Shimodaira, H. (2000). Improving predictive inference under covariate shift by weighting the log-likelihood function. *Journal of Statistical Planning and Inference*, 90.

- Song, H. and Raskutti, G. (2019). PUlasso: High-dimensional variable selection with presence-only data. *Journal of the American Statistical Association*, 115.
- Sugiyama, M., Krauledat, M., and Müller, K.-R. (2007). Covariate shift adaptation by importance weighted cross validation. *Journal of Machine Learning Research*, 8.
- Tian, Q., Zhang, X., and Zhao, J. (2023). ELSA: Efficient label shift adaptation through the lens of semiparametric models. In *International Conference on Machine Learning*.
- Wang, L., Schnall, J., Small, A., Hubbard, R. A., Moore, J. H., Damrauer, S. M., and Chen, J. (2021). Case contamination in electronic health records based case-control studies. *Biometrics*, 77.
- Ward, G., Hastie, T., Barry, S., Elith, J., and Leathwick, J. R. (2009). Presence-only data and the EM algorithm. *Biometrics*, 65.